

High-density one-dimensional well-aligned germanium quantum dots on a nanoridge array

Yan-Ru Chen,¹ Chieh-Hsiung Kuan,^{1,a)} Yuen-Wuu Suen,^{2,3,b)} Yu-Hwa Peng,⁴
Peng-Shiu Chen,⁵ Cha-Hsin Chao,⁶ Eih-Zhe Liang,⁶ Ching-Fuh Lin,^{1,6} and Hung-Chun Lo⁷

¹Graduate Institute of Electronics Engineering and Department of Electrical Engineering,
National Taiwan University, Taipei, Taiwan

²Department of Physics, National Chung Hsing University, Taichung, Taiwan

³Institute of Nanosciences, National Chung Hsing University, Taichung, Taiwan

⁴Department of Electronics Engineering, Lan Yang Institute of Technology, Yilan, Taiwan

⁵Department of Materials Science and Engineering, Ming Hsin University of Science and Technology,
Hsinchu, Taiwan

⁶Institute of Electro-Optical Engineering, National Taiwan University, Taipei, Taiwan

⁷Department of Material Science and Engineering, National Chiao Tung University, Hsinchu, 300 Taiwan

(Received 8 May 2008; accepted 7 August 2008; published online 26 August 2008)

The selective growth of high-density one-dimensional well-aligned Ge quantum dots (QDs) on the top of nanoridges patterned on Si substrate is reported. The period of ridge array is 150 nm, the width of each ridge is 80 nm, and the depth of the trench is 20 nm. The areal density of QDs is about $5.4 \times 10^9 \text{ cm}^{-2}$. Simulations of the chemical potential show that a proper distribution of the surface curvature may give rise to a suitable chemical potential minimum helping positioning the QDs. These ridges can also be used to control the shape and the uniformity of QDs. © 2008 American Institute of Physics. [DOI: 10.1063/1.2976549]

Preferential growth of self-assembled germanium (Ge) quantum dots (QDs) on silicon (Si) substrates is of special interest because of its potential applications to electronic and optoelectronic devices.^{1,2} In the growth process, after wetting layer deposition Ge QDs are formed and the misfit strain³ is relaxed at the same time; they nucleate at random positions and exhibit a rather large size dispersion.⁴ However, the size, density and position of Ge QDs are very critical to realistic device applications.⁵ Recently, major progresses on improving the spatial alignment and the uniformity of Ge QDs have been achieved by integration of lithography and self-assembling growth techniques.^{6–12} Most of these works demonstrated that QDs were grown in trenches, or pits, with concave surfaces,^{7–13} only in few of them QDs were on the ridges, which are convex surfaces.^{6,7,12,13} They have shown that selective growth on the top of ridge can be achieved by a wetting layer with a higher Ge concentration which may relax the misfit strain,^{7,12} by corrugative hill patterns on Si substrates which modify the elastic energy of QDs,¹³ or by a thin oxide layer⁶ which covers the trench part. Here, we demonstrate the selective growth of Ge QDs only on the top of ridges of nanometer scale. High-density one-dimensional (1D) well-aligned Ge QDs can be obtained by integrating lithography, etching, and deposition systems. The size of QDs can also be controlled by the width of ridge. Simulations taking chemical potential and surface profile into consideration show that a large surface curvature may yield a local chemical potential minimum on the top of nanoridges, which is necessary for the growth of Ge QDs thereat. Our results can be applied to form the active QDs in nanocrystal nonvolatile memories¹ and high efficient QD infrared detectors.²

The QD locations are determined via the mass transport process controlled by the chemical potential: atoms diffuse from regions of high chemical potential to regions of lower chemical potential.¹⁴ Chemical potential is the sum of surface energy and strain energy. Manipulation of the curvature of the Si surface may give rise to a local potential minimum on the top of a ridge, where the QD has more chance to nucleate. To find the morphology which results in a 1D QD growth, we fabricated several periodic nanoridge arrays with various surface curvatures and deposited Ge QDs on them.

The periodic nanoridges on a Si substrate with various surface curvatures are patterned with e-beam lithography and reactive ion etching. A wetting layer is deposited and then Ge QDs are grown in an ultrahigh vacuum chemical vapor deposition system. The substrate temperature is maintained at 600 °C during growth. The nominal thickness of Ge layer is 7 ML (monolayer). The surface morphology is investigated by an atomic force microscope (AFM) afterward. Figure 1(a) shows the AFM image of a sample (marked as sample A) with all Ge QDs being deposited only on the top of ridges, but not in the trenches. The fabrication parameters are listed in Table I. The distance between each line of QDs is 150 nm, the same as the period of the host Si template with an 80-nm-wide ridge array. The depth of the trenches is about 20 nm. The solid line in Fig. 1(b) illustrated the profile across a ridge with a 10 nm Si_{0.8}Ge_{0.2} wetting layer. Please notice that unlike the prior work,⁶ the trenches here are not protected by an oxide layer. The areal density of Ge QDs is estimated to be $5.4 \times 10^9 \text{ cm}^{-2}$, which is the highest for Ge QDs 1D array grown on the top of ridges ever reported in literature.^{6,8,9,12}

To understand the spatial distribution of Ge QDs, we can examine the chemical potential determining the growth of Ge QDs, following the model given by Yang *et al.*¹² The chemical potential, μ , can be written as

^{a)}Electronic mail: kuan@cc.ee.ntu.edu.tw.

^{b)}Electronic mail: ysuen@phys.nchu.edu.tw.

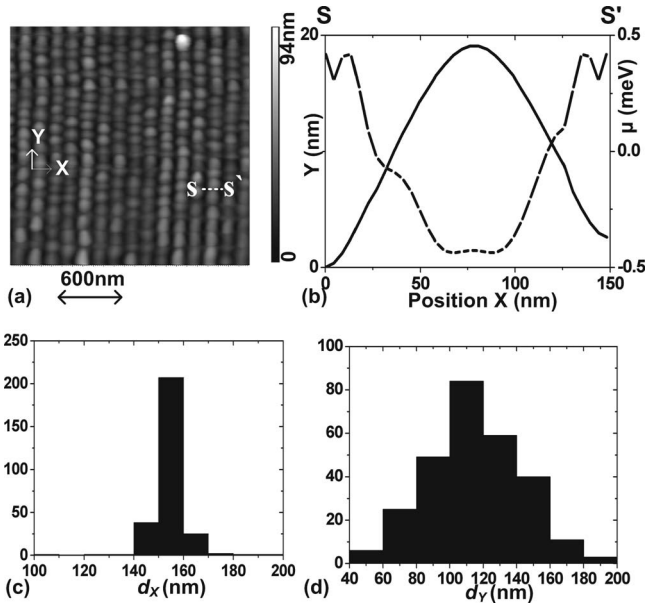


FIG. 1. (a) AFM picture of sample A. X and Y axes indicate the directions perpendicular and parallel to the direction of ridge array, respectively. (b) Calculated local chemical potential (dashed line) along S - S' in (a). The solid line is the AFM-investigated surface profile. [(c) and (d)] Histograms of d_x and d_y . Data are collected from 277 dots.

$$\mu = \mu_0 + \Omega \gamma \kappa + \Omega E_s, \quad (1)$$

where μ_0 is the chemical potential for a flat surface, Ω is the atomic volume, γ is the surface free energy per unit area, k is the surface curvature, and E_s is the local strain relaxation energy. The curvature k is

$$\kappa = -z''[1 + (z')^2]^{-3/2}, \quad (2)$$

with z being the height of the surface along the normal to the surface plane, z' and z'' being the first and second derivatives with respect to x , respectively, and x being the position along the surface plane. The change of local chemical potential due to morphology comprises the surface energy $\Omega \gamma \kappa$ and the strain energy ΩE_s . The local strain relaxation energy relative to a flat film, E_s , can be formulated by¹²

$$E_s = -\frac{C}{2} \left(\frac{\kappa}{|\kappa|} [\kappa(z_s - z_0)]^2 - \varepsilon^2 \right), \quad (3)$$

where C is the elastic constant, z_s is the position of the top surface, z_0 is the position of the neutral plane of the bent film, and ε is the misfit strain between QDs and the wetting layer. Here it is assumed that the wetting layer conforms exactly to the shape of the underlying patterned Si template,¹² and the Ge QD on the surface of wetting layer is treated as a bent film.¹⁵ The quantity $(z_s - z_0)$ represents the average displacement of the bent film and is treated as a

TABLE I. Fabrication parameters of samples A–C.

Sample	Sample A	Samples B and C
Period	150 nm ~80 nm	800 and 600 nm
Ridge width	(full width at half maximum)	~320 and ~200 nm
Height of ridges	~20 nm	~60 nm
Growth rate	0.1 nm/s	0.1 nm/s
Wetting layer	10 nm Si _{0.8} Ge _{0.2}	20 nm Si

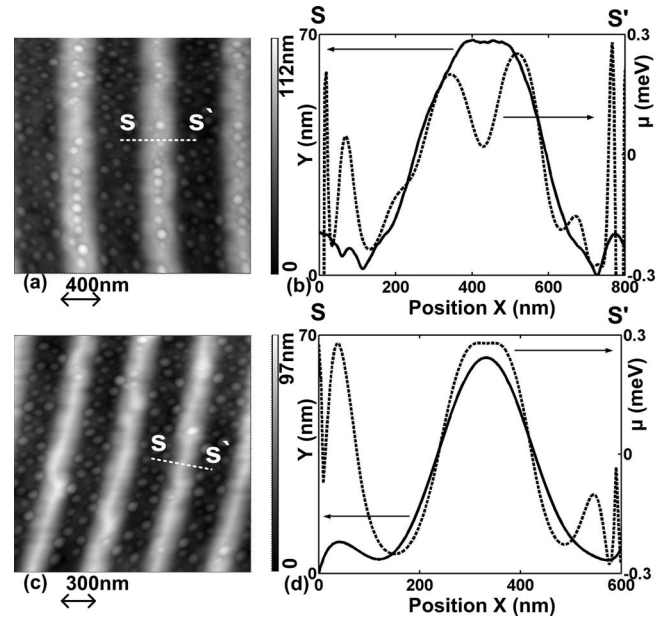


FIG. 2. (a) AFM picture of sample B. (b) Calculated local chemical potential (dashed line) along S - S' in (a). The solid line is the AFM-investigated surface profile. (c) AFM picture of sample C. (d) Calculated local chemical potential (dashed line) along S - S' in (c). The fitting parameter ($z_s - z_0$) here is 1.5 nm.

fitting parameter, which is chosen to give a minimum μ in a selective area and correct QD positions. The surface curvature, k , in convex regions is positive, and in concave regions is negative. Thus, according to Eq. (1), k of the top of a nanoridge would make a positive contribution to surface energy, but a negative contribution to strain energy. To grow Ge QDs specifically right on the top of a ridge, the local strain energy has to be negative enough to overcome the surface energy, yielding a local chemical potential minimum there. To achieve this, two possible methods can be employed: one is to decrease ε due to misfit through a suitable wetting layer,^{7,12} and the other is to engineer the surface curvature, κ .^{12,13} Since the surface energy is to the first order of k , while the strain energy is to the second order of k , for a large enough k , corresponding to a ridge with narrow enough width, the magnitude of the strain energy could surpass the surface energy term.

The simulated distribution of chemical potential across a ridge in sample A is illustrated in Fig. 1(b). The measured surface profile, the solid-line curve in Fig. 1(b), along the white dashed line S - S' across the ridge without QD in Fig. 1(a) is used to estimate k via Eq. (2). The result shows a remarkable local chemical potential minimum with a broad basin lying exactly on the top of the nanoridge, consistent with the positions of Ge QDs. Note that the zero value of μ corresponds to a flat surface with $k=0$. The fitting parameter ($z_s - z_0$) is chosen to be 1.2 nm.

In contrast with sample A, we fabricated two test samples, B and C, with ridges of wider widths. Besides the size of the template ridges and the wetting layer, these samples have similar fabrication process and parameters, which are also listed in Table I. The AFM picture of sample B in Fig. 2(a) shows that the Ge QDs are grown not only on the top of ridges but also in the trenches, compared with Fig. 2(c) for sample C, which shows very few QDs are on the ridges. Figures 2(b) and 2(d) illustrate the simulated chemi-

cal potential distributions across a ridge for samples B and C, respectively, together with their measured surface profiles by AFM. The concordance between the distribution of chemical potential and the Ge QDs is evident: the potential minimum on the top of the ridge relative to the trench regime for sample B is deeper than that of sample C, yet much shallower than that of sample A, resulting in the corresponding distributions of QDs for these samples.

Finally, the size of QDs and its standard variation are found to be drastically affected by the nanoridge array. From the AFM data of sample A in Fig. 1(a), the average dimension perpendicular to the ridge (d_x) of the Ge QDs is 152 nm with a standard variation (σ) of 6 nm, while the size along the ridge (d_y) is 109 nm with $\sigma=28$ nm. Figures 1(c) and 1(d) show the histograms for d_x and d_y of Ge QDs. Apparently, not only d_x is enlarged by the ridge but the σ is also suppressed. Similarly, the AFM data of the QDs on the top of ridges for sample B in Fig. 2(a) give $d_x=104$ nm, larger than $d_y=88$ nm; however, σ is about 20 nm for both directions, no variation suppression being observed. Even though no detailed microscopic model can be provided so far for this effect, the small value of σ for d_x can be attributed to the relatively deep and broad potential minimum for sample A illustrated in Fig. 1(b) compared to the shallower and narrower minimum for sample B in Fig. 2(b). We also notice that the shapes of the QDs on the top of ridges are all dome-like, in contrast with the QDs in the trench or in samples without ridge patterns having both dome-like and pyramid-like shapes. The narrow ridge can be used to inhibit bimodal growth of Ge QDs.⁶ Similar results on shape and uniformity control of Ge QDs in the trench (or trough) region are discussed in Ref. 13. Our results suggest that the uniformity and also the shape of Ge QDs on top of ridges can be controlled by nanopatterning.

In conclusion, high-density 1D well-aligned Ge QDs selectively grown on the top of nanoridges patterned on a Si substrate are experimentally achieved by carefully designing the distribution of the surface curvature, which may give rise to a suitable chemical potential minimum helping positioning the QDs. The same method can also be used to control the growth mode and the uniformity of QDs on nanoridges.

This work was supported by the NTU Center for Information and Electronics Technologies for the *E*-beam system and National Science Council of the Republic of China under Contract Nos. NSC-96-2120-M-009-010 and NSC-96-2628-E-002-250-MY3.

- ¹K. I. Han, Y. M. Park, S. Kim, S. H. Choi, K. J. Kim, I. H. Park, and B. G. Park, *IEEE Trans. Electron Devices* **54**, 359 (2007).
- ²B.-C. Hsu, S. T. Chang, T.-C. Chen, P.-S. Kuo, P. S. Chen, Z. Pei, and C. W. Liu, *IEEE Electron Device Lett.* **24**, 318 (2003).
- ³I. Berbezier and A. Ronda, *Phys. Rev. B* **75**, 195407 (2007).
- ⁴R. E. Rudd, G. A. D. Briggs, A. P. Sutton, G. Medeiros-Ribeiro, and R. S. Williams, *Phys. Rev. Lett.* **90**, 146101 (2003).
- ⁵X. Q. Li, H. Nakayama, and Y. Arakawa, *Phys. Rev. B* **59**, 5069 (1999).
- ⁶G. Jin, J. L. Liu, S. G. Thomas, Y. H. Luo, K. L. Wang, and B.-Y. Nguyen, *Appl. Phys. Lett.* **75**, 2752 (1999).
- ⁷Z. Zhong, A. Halilovic, M. Mühlberger, F. Schäffler, and G. Bauer, *J. Appl. Phys.* **93**, 6258 (2003).
- ⁸Z. Zhong and G. Bauer, *Appl. Phys. Lett.* **84**, 1922 (2004).
- ⁹G. S. Kar, S. Kiravittaya, M. Stoffel, and O. G. Schmidt, *Phys. Rev. Lett.* **93**, 246103 (2004).
- ¹⁰A. Karmous, A. Cuenat, A. Ronda, I. Berbezier, S. Atha, and R. Hull, *Appl. Phys. Lett.* **85**, 6401 (2004).
- ¹¹S. Watanabe, E. Pelucchi, B. Dwir, M. H. Baier, K. Leifer, and E. Kapon, *Appl. Phys. Lett.* **84**, 2907 (2004).
- ¹²B. Yang, F. Liu, and M. G. Lagally, *Phys. Rev. Lett.* **92**, 025502 (2004).
- ¹³G. Chen, G. Vastola, H. Lichtenberger, D. Pachinger, G. Bauer, W. Jantsch, F. Schäffler, and L. Miglio, *Appl. Phys. Lett.* **92**, 113106 (2008).
- ¹⁴R. V. Kukta and D. Kouris, *J. Appl. Phys.* **97**, 033527 (2005).
- ¹⁵F. Liu, M. Huang, P. P. Rugheimer, D. E. Savage, and M. G. Lagally, *Phys. Rev. Lett.* **89**, 136101 (2002).